Nonlocal Contributions to Degenerate Four-Wave Mixing in Noncentrosymmetric Materials

Ivan Biaggio

Nonlinear Optics Laboratory, Institute of Quantum Electronics, Swiss Federal Institute of Technology, ETH-Hönggerberg, CH-8093 Zürich, Switzerland

(Received 11 September 1998)

Cascaded second-order and piezoelectric contributions to degenerate four-wave mixing in noncentrosymmetric materials are analyzed in detail. The effective third-order susceptibility measured in degenerate four-wave mixing becomes strongly dependent on experimental parameters that do not normally influence the third-order response in centrosymmetric materials. This introduces important new requirements for reliable reporting of experimental results. A new technique that allows us to experimentally relate the third-order susceptibility to the high-frequency electro-optic and dielectric properties is introduced and demonstrated in $BaTiO_3$ and $KNbO_3$. [S0031-9007(98)08117-4]

PACS numbers: 78.20.Bh, 42.65.Hw, 77.65.–j, 77.84.–s

Pulsed degenerate four-wave mixing (DFWM) is a widespread tool for characterizing third-order susceptibilities of candidate materials for nonlinear optical applications. We discuss important second-order effects that cause unexpected geometrical and pulse-length dependencies of the DFWM signal. They are due to the concurrent processes of optical rectification and linear electro-optic effect, and to piezoelectric elastic relaxation. If neglected, these "cascaded" second-order effects can lead to misleading DFWM results in noncentrosymmetric materials. In this Letter we give the first complete expressions to calculate their contributions to the DFWM signal, and show how they can be used to relate experimentally the third-order susceptibility to the linear electro-optic and dielectric properties.

We first point out the origin of second-order contributions and give general equations for calculating them for the most important DFWM setups, correcting and completing some expressions given in Ref. [1]. We then discuss the piezoelectric relaxation of the crystal as it is constrained by the boundary conditions defined by the DFWM experimental geometry, and calculate the effective electro-optic and dielectric tensors to be used when relaxation to a new elastic configuration is possible. Last, we demonstrate experimentally, in the well known electro-optic materials $BaTiO_3$ and $KNbO_3$, how these results can be used to obtain absolute third-order susceptibilities by comparing to independently determined electro-optic and dielectric properties, without using a reference material.

We start with the definition of the third-order nonlinear optical susceptibilities. Consider an electric field that is a sum of three plane waves with wave vectors $\mathbf{k}_i$ and frequency ω,

$$\mathbf{E}(\mathbf{r},t) = \frac{1}{2}\sum_{n=1}^{3}\mathbf{E}_n(\omega,\mathbf{k}_n)\exp[i(\mathbf{k}_n\mathbf{r} - \omega t)] + \text{c.c.}, \quad (1)$$

where the $\mathbf{E}_n(\omega,\mathbf{k}_n)$ are the complex amplitudes of the three input waves, which can be distinguished by their wave vectors. In case of pulsed experiments, Eq. (1) describes the field in a time interval much shorter than the laser pulses, which we consider so long that an "instantaneous" response can be safely assumed.

The field of (1) induces a time-dependent third-order polarization [2,3],

$$P_l^{(3)}(\mathbf{r},t) = \epsilon_0\chi_{ijkl}^{(3)} \cdot E_i(\mathbf{r},t)E_j(\mathbf{r},t)E_k(\mathbf{r},t), \quad (2)$$

where $\chi_{ijkl}^{(3)}$ is the third-order nonlinear optical susceptibility in the time domain, ϵ_0 is the permittivity of vacuum, and we use SI units. Summation over repeated indices is understood.

Figure 1 shows two ways of arranging the three input waves so that the nonlinear polarization at frequency ω and wave vector $\mathbf{k}_4 = \mathbf{k}_1 + \mathbf{k}_2 - \mathbf{k}_3$, with complex amplitude $\mathbf{P}(\omega,\mathbf{k}_4)$, radiates the signal wave in a phase matched way over the whole sample thickness. Inserting

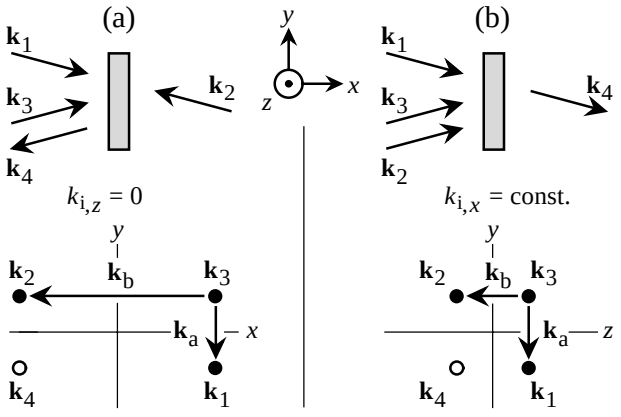

FIG. 1. Two common DFWM experimental geometries. Three beams with wave vectors $\mathbf{k}_1$, $\mathbf{k}_2$, and $\mathbf{k}_3$ interact in a sample to generate a fourth beam with wave vector $\mathbf{k}_4$. The interacting beams and the sample are drawn in the x-y plane in the first line, and the coordinates of the beam wave vectors are plotted in the second line. For clarity, the x and y axes are not in scale. (a) Beams 1 and 2, and beams 4 (signal) and 3, are counterpropagating [4]. (b) All input beams travel towards the positive x direction. The beams are distinguished by a slightly different z direction [5].

(1) into (2), and collecting the terms with frequency ω and wave vector $\mathbf{k}_4$, one finds

$$P_l(\omega,\mathbf{k}_4) = \tfrac{3}{2}\epsilon_0\chi^{(3)}_{ijkl}(\omega,\omega,-\omega,-\omega,\mathbf{k}_1,\mathbf{k}_2,-\mathbf{k}_3,-\mathbf{k}_4) \times E_i(\omega,\mathbf{k}_1)E_j(\omega,\mathbf{k}_2)E^*_k(-\omega,-\mathbf{k}_3)\,. \quad (3)$$

$\chi^{(3)}_{ijkl}(\omega,\omega,-\omega,-\omega,\mathbf{k}_1,\mathbf{k}_2,-\mathbf{k}_3,-\mathbf{k}_4)$ is the third-order optical susceptibility tensor that describes DFWM [4].

Our SI expressions use the same convention as in Ref. [6]. They go over to the ones in electrostatic units (*e.s.u.*) of Refs. [2,3], used in a relevant part of the literature, with the substitution $\epsilon_0\chi^{(3)}_{ijkl} \leftrightarrow 4c_{ijkl}$, while numerical values are converted using the rule

$$\chi^{(3)}_{ijkl}[\mathrm{m}^2\,\mathrm{V}^{-2}] = 4\,\frac{4\pi}{(10^{-4}c)^2}\,c_{ijkl}[e.s.u.], \quad (4)$$

where c is the speed of light in vacuum in m/s. This takes into account the additional factor (1/4) that was included in the definition of the third-order susceptibilities c_{ijkl} [2].

In a noncentrosymmetric material, the field of (1) also leads to a second-order polarization. The only part that gives a large phase matched contribution to DFWM is induced by optical rectification, and it consists of the sum of two components oscillating in space like a plane wave. Their complex amplitudes are

$$P^{(\mathrm{OR})}_p(\omega=0,\mathbf{k}_a=\mathbf{k}_1-\mathbf{k}_3) = \epsilon_0\chi^{(2)}_{ikp}(\omega,-\omega,0,\mathbf{k}_1,-\mathbf{k}_3,-\mathbf{k}_a)E_i(\omega,\mathbf{k}_1)E^*_k(-\omega,-\mathbf{k}_3) \quad (5)$$

and

$$P^{(\mathrm{OR})}_p(\omega=0,\mathbf{k}_b=\mathbf{k}_2-\mathbf{k}_3) = \epsilon_0\chi^{(2)}_{jkp}(\omega,-\omega,0,\mathbf{k}_2,-\mathbf{k}_3,-\mathbf{k}_b)E_j(\omega,\mathbf{k}_2)E^*_k(-\omega,-\mathbf{k}_3)\,. \quad (6)$$

These two polarizations are induced by two pairs of input waves. They interact with the remaining input wave in (1) to generate a nonlinear polarization of exactly the same form as (3), with frequency ω and wave vector $\mathbf{k}_4$:

$$P^{\mathrm{casc}}_l(\omega,\mathbf{k}_4) = \epsilon_0\chi^{(2)}_{pjl}(0,\omega,-\omega,\mathbf{k}_a,\mathbf{k}_2,-\mathbf{k}_4)\left[\frac{P^{\mathrm{OR}}_p(\mathbf{k}_a)}{\epsilon_0(\epsilon_{pp}+2)}+E^{\mathrm{OR}}_p(\mathbf{k}_a)\right]E_j(\omega,\mathbf{k}_2) + \epsilon_0\chi^{(2)}_{pil}(0,\omega,-\omega,\mathbf{k}_b,\mathbf{k}_1,-\mathbf{k}_4)\left[\frac{P^{\mathrm{OR}}_p(\mathbf{k}_b)}{\epsilon_0(\epsilon_{pp}+2)}+E^{\mathrm{OR}}_p(\mathbf{k}_b)\right]E_i(\omega,\mathbf{k}_1)\,. \quad (7)$$

The factor $\epsilon_{ii}+2$ has been discussed by Flytzanis and Bloembergen [7]. It is obtained in the Lorenz local field approximation by relating to the microscopic (local) electric field induced by the polarization.

$\mathbf{E}^{\mathrm{OR}}(\mathbf{k})$ is the macroscopic electric field that can be induced by the polarization $\mathbf{P}^{\mathrm{OR}}(\mathbf{k}) = \mathbf{P}^{\mathrm{OR}}(\omega=0,\mathbf{k})$ in (5) and (6). For laser pulses so long that time varying magnetic fields can be neglected, $\mathbf{E}^{\mathrm{OR}}(\mathbf{k})$ must be curl-free. Through the linear susceptibility, it induces a polarization that must be added to $\mathbf{P}^{\mathrm{OR}}$ to get the displacement field $D_i = \epsilon_0\epsilon_{ij}E^{\mathrm{OR}}_j + P^{\mathrm{OR}}_i$, which must be divergence-free in the absence of free charges. From rot $E^{\mathrm{OR}} = 0$ and div $\mathbf{D} = 0$ we obtain

$$\mathbf{E}^{\mathrm{OR}}(\mathbf{k}) = -\mathbf{k}\,\frac{k_iP^{\mathrm{OR}}_i(\mathbf{k})}{\epsilon_0\epsilon_{ij}k_ik_j}\,. \quad (8)$$

It is useful to separate $\mathbf{P}^{\mathrm{OR}}$ in a transversal part with zero divergence and $\mathbf{P}^{\mathrm{OR}}(\mathbf{k}) \perp \mathbf{k}$, and a longitudinal part with zero curl and $\mathbf{P}^{\mathrm{OR}}(\mathbf{k}) \parallel \mathbf{k}$. $\mathbf{E}^{\mathrm{OR}} = 0$ for a transversal polarization, and $E^{\mathrm{OR}}_i = -P^{\mathrm{OR}}_i/(\epsilon_0\epsilon_{ii})$ for a longitudinal polarization oriented parallel to a main axis of the dielectric tensor.

In a DFWM experiment, the contributions from (3) and (7) add. By combining (7) with (5) and (6), and comparing to (3), we can define an effective susceptibility that must replace $\chi^{(3)}_{ijkl}$ in (3) whenever a noncentrosymmetric material is used:

$$\chi^{(3),\mathrm{EFF}}_{ijkl} = \chi^{(3)}_{ijkl} + \chi^{\mathrm{casc},\mathbf{k}_a}_{ijkl} + \chi^{\mathrm{casc},\mathbf{k}_b}_{ijkl}\,. \quad (9)$$

$\chi^{\mathrm{casc},\mathbf{k}_a}_{ijkl}$ and $\chi^{\mathrm{casc},\mathbf{k}_b}_{ijkl}$ describe the cascaded contributions and depend on the wave vector differences $\mathbf{k}_a = \mathbf{k}_1 - \mathbf{k}_3$ and $\mathbf{k}_b = \mathbf{k}_2 - \mathbf{k}_3$, via (5)–(8). They can be calculated in a more compact form by relating the second-order susceptibilities appearing in (5)–(7) to the electro-optic coefficients $r_{ijk} = r_{jik}$ describing the change of the optical indicatrix by an electric field $\mathbf{E}$ as $\Delta(1/\epsilon)_{ij} = r_{ijk}E_k$:

$$\chi^{(2)}_{ijk}(\omega,-\omega,0) = -\tfrac{1}{2}n_i^2n_j^2r_{ijk}\,, \quad (10)$$

where the n_i are the refractive indices at frequency ω, and $\chi^{(2)}_{kij}(0,\omega,-\omega) = \chi^{(2)}_{ijk}(\omega,-\omega,0)$.

We can now write $\chi^{\mathrm{casc},\mathbf{k}_a}_{ijkl}$ and $\chi^{\mathrm{casc},\mathbf{k}_b}_{ijkl}$ for $\mathbf{k}_a$ and $\mathbf{k}_b$ parallel to a main axis of the dielectric tensor. For $\mathbf{P}^{(\mathrm{OR})}(\omega=0,\mathbf{k}) \perp \mathbf{k}$ (transversal polarization),

$$\chi^{\mathrm{casc},\mathbf{k}_a}_{ijkl} = \frac{1}{6}\,\frac{n_i^2n_j^2n_k^2n_p^2r_{ikp}r_{jlp}}{\epsilon_{pp}+2}\,, \quad (11)$$

$$\chi^{\mathrm{casc},\mathbf{k}_b}_{ijkl} = \frac{1}{6}\,\frac{n_i^2n_j^2n_k^2n_p^2r_{jkp}r_{ilp}}{\epsilon_{pp}+2}\,. \quad (12)$$

For $\mathbf{P}^{(\mathrm{OR})}(\omega=0,\mathbf{k}) \parallel \mathbf{k}$ (longitudinal polarization),

$$\chi^{\mathrm{casc},\mathbf{k}_a}_{ijkl} = -\frac{1}{3}\,\frac{1}{\epsilon_{pp}}\,\frac{n_i^2n_j^2n_k^2n_p^2r_{ikp}r_{jlp}}{\epsilon_{pp}+2}\,, \quad (13)$$

$$\chi^{\mathrm{casc},\mathbf{k}_b}_{ijkl} = -\frac{1}{3}\,\frac{1}{\epsilon_{pp}}\,\frac{n_i^2n_j^2n_k^2n_p^2r_{jkp}r_{ilp}}{\epsilon_{pp}+2}\,. \quad (14)$$

For high dielectric constants these last "longitudinal" contributions are negligible. But in low-dielectric constant materials such as molecular crystals they can remain comparable to the direct third-order susceptibility.

In (11)–(14), r_{ijk} and ϵ_{ij} are electro-optic and dielectric tensors at constant strain when short enough pulses are used, but they are effective tensors including acoustic

phonon contributions when the spatial periods $2\pi/k_a$ or $2\pi/k_b$ are so small that elastic deformations can build up during the laser pulse length. This can already be the case for 100 ps pulses for one of the contributions of Fig. 1a: $2\pi/k_b$ can reach 0.1 μm inside the crystal for a light wavelength of $\sim$0.5 μm, and an acoustic wave with a speed of 5 km/s travels that distance in 20 ps.

These effective tensors are not simply the directly measurable ones at constant stress (unclamped) because only certain acoustic phonon contributions are allowed. The electric and strain fields in the crystal must have in our case a plane-wave spatial dependence $\mathbf{E}(\mathbf{k}) = \mathbf{E}\exp(i\mathbf{kx})$ and $\mathbf{u}(\mathbf{k}) = \mathbf{u}\exp(i\mathbf{kx})$ with the complex (vectorial) amplitudes $\mathbf{E}$ and $\mathbf{u}$. This boundary condition breaks the symmetry of the crystal, leading to modified, wave vector dependent r_{ijk} and ϵ_{ij} tensors with a lower symmetry. A similar problem has been treated in Ref. [8] assuming an electric field always parallel to the modulation wave vector. In our case the rectified polarization can also be perpendicular to the wave vectors $\mathbf{k}_a$ and $\mathbf{k}_b$, and we need to treat the problem in general by looking at the general relationships between electric field, strain, and dielectric tensor. The electro-optic tensor r^S_{ijk} at constant strain and the elasto-optic tensor p^E_{ijkl} at constant electric field determine the change in the dielectric tensor induced by the spatially sinusoidal electric and strain fields,

$$\Delta\epsilon^{-1}_{ij}(\mathbf{k}) = r^S_{ijk}E_k(\mathbf{k}) + p^E_{ijkl}u_{kl}(\mathbf{k}), \qquad (15)$$

where $u_{kl}(\mathbf{k}) = \partial u_k(\mathbf{k})/\partial x_l$.

By calculating $\mathbf{u}(\mathbf{k})$ from $\mathbf{E}(\mathbf{k})$, we can relate the amplitude of the dielectric tensor modulation (15) to the amplitude of the electric field modulation $\mathbf{E}$ with an effective electro-optic tensor r_{ijk} defined by $\Delta\epsilon^{-1}_{ij} = r_{ijk}E_k$.

The stress tensor T_{ij} can be expressed as a function of the strain tensor $S_{kl} = (u_{kl} + u_{lk})/2$ and the electric field by means of the elastic stiffness tensor at constant electric field C^E_{ijkl} and the piezoelectric tensor e_{ijk}:

$$T_{ij}(\mathbf{k}) = C^E_{ijkl}S_{kl}(\mathbf{k}) - e_{mij}E_m(\mathbf{k}). \qquad (16)$$

For a static deformation the divergence of the stress tensor $\partial T_{ij}/\partial x_j$ must vanish [9]. Since all spatial dependencies are in the form of a plane wave, taking the divergence leads to an algebraic equation relating the amplitudes of the strain field and the electric field,

$$C^E_{ijkl}\hat{\kappa}_j u_k \hat{\kappa}_l = E_m e_{mij}\hat{\kappa}_j/k, \qquad (17)$$

with k the modulus of the wave vector $\mathbf{k}$ and $\hat{\kappa}_i = k_i/k$.

Defining $A_{ik} = C^E_{ijkl}\hat{\kappa}_j\hat{\kappa}_l$ and $b_i = E_m e_{mij}\hat{\kappa}_j/k$, and substituting in (17), reveals the system of three linear inhomogenous equations $A_{ik}u_k = b_i$. The matrix A_{ik} is symmetric and can be inverted [9] to obtain the solution $u_k = A^{-1}_{ki}b_i$, which is then inserted in (15) to get the effective electro-optic coefficient we were looking for,

$$r_{ijk}(\mathbf{k}) = r^S_{ijk} + p_{ijmn}e_{klu}\hat{\kappa}_n\hat{\kappa}_u(A^{-1})_{ml}. \qquad (18)$$

The dielectric tensor at constant strain ϵ^S_{ij} and the piezoelectric tensor e_{ijk} determine the displacement field $D_i(\mathbf{k}) = \epsilon_0\epsilon^S_{ij}E_j(\mathbf{k}) + e_{ijk}S_{jk}(\mathbf{k})$. Inserting $u_k = A^{-1}_{ki}b_i$ from (17) we obtain $D_i = \epsilon_0\epsilon_{ij}E_j$ for the modulation amplitudes, with the effective dielectric tensor

$$\epsilon_{ij}(\mathbf{k}) = \epsilon^S_{ij} + \frac{1}{\epsilon_0}\hat{\kappa}_n\hat{\kappa}_k e_{imk}e_{jln}(A^{-1})_{ml}. \qquad (19)$$

Equations (18) and (19) must be used in (11)–(14) whenever elastic deformations can be established during the laser pulse length. Note the symmetry breaking induced by the presence of the wave vector $\mathbf{k}$. The effective tensors (18) and (19) belong in general to a lower symmetry, e.g., orthorhombic instead of tetragonal for $\mathbf{k}$ along the 1 axis in $BaTiO_3$ (where the 1 and 2 axes are otherwise equivalent).

In centrosymmetric materials, any coefficient $\chi^{(3)}_{ijkl}$ defined in (3) can be measured in DFWM by appropriately choosing the polarizations of the three input beams and the signal beam in the sample reference frame.

This is not true for noncentrosymmetric materials. Even when the polarizations are kept constant in the sample reference frame, the second-order nonlocal contributions depend on the wave vector differences $\mathbf{k}_a$ and $\mathbf{k}_b$, and change with sample orientation, DFWM setup, and pulse length.

To fix the ideas, we calculate the influence of these parameters for tetragonal $BaTiO_3$ and orthorhombic $KNbO_3$. We use the r^S_{ijk} extrapolated at 1.06 μm [10], and Refs. [8] and [11] for the other material constants.

The separate contributions from $\mathbf{P}^{\mathrm{OR}}(\mathbf{k}_a)$ and $\mathbf{P}^{\mathrm{OR}}(\mathbf{k}_b)$ are shown in Table I for the two DFWM geometries of Fig. 1 and two orientations of the polar 3-axis of the crystals (labeled c). All light polarizations are kept constant in the sample reference frame, and the direct third-order contributions do not change with crystal orientation or experimental setup. The cascaded contributions, on the other hand, vary considerably. As an example, $\chi^{(3)}_{3333}$ can be measured with (i) $c \parallel y$ and all beams polarized along y, or (ii) $c \parallel z$ and all beams polarized along z (the angles between the beams can always be chosen so small that the x components of the optical electric field are negligible). For $\chi^{(3)}_{3333}$ only r_{333} contributes to $\mathbf{P}^{\mathrm{OR}}$, which is

TABLE I. Cascaded contributions from the rectified polarizations with wave vectors $\mathbf{k}_a$ and $\mathbf{k}_b$, calculated from (11)–(14) in units of 10^{-22} m^2/V^2 for two possible orientations of the c axis and the two DFWM setups shown in Fig. 1.

			Fig. 1a		Fig. 1b	
		c	$\mathbf{k}_a$	$\mathbf{k}_b$	$\mathbf{k}_a$	$\mathbf{k}_b$
$KNbO_3$	$\chi^{\mathrm{casc}}_{3333}$	y	-2	36.6	-2	24.3
		z	24.3	36.6	24.3	-2
	$\chi^{\mathrm{casc}}_{2233}$	y	135	135	135	-0.3
		z	-0.3	135	-0.3	135
$BaTiO_3$	$\chi^{\mathrm{casc}}_{3333}$	y	-0.9	24.2	-0.9	24.5
		z	24.5	24.2	24.5	-0.9
	$\chi^{\mathrm{casc}}_{1133}$	y	224	224	-0.2	224
		z	-0.2	224	224	-0.2

then parallel to c. For the setup in Fig. 1a, both rectified polarizations are transversal for $c \parallel z$, while $\mathbf{P}^{\mathrm{OR}}(\mathbf{k}_a)$ becomes longitudinal for $c \parallel y$. For the Fig. 1b setup, $\mathbf{P}^{\mathrm{OR}}(\mathbf{k}_a)$ is transversal and $\mathbf{P}^{\mathrm{OR}}(\mathbf{k}_b)$ longitudinal for $c \parallel z$, and vice versa for $c \parallel y$. To give an example of its effect, we include piezoelectric elastic relaxation for the contribution with the large wave vector $\mathbf{k}_b$ in Fig. 1a. All other cascaded contributions were calculated using the clamped (strain-free) coefficients, and are valid up to laser pulse lengths of several nanoseconds, depending on the angle between the beams. The same reasoning can be applied to $\chi^{(3)}_{1133}$ and $\chi^{(3)}_{2233}$, but here the piezoelectric contribution for $\mathbf{k}_{a,b} \perp c$ always vanishes by symmetry, as can be demonstrated with (18).

Despite the fact that direct third-order contributions are identical for every pair of rows of Table I, the total cascaded contributions can differ by a factor of ~ 2. They are different for the two experimental setups of Fig. 1 and change with sample orientation in the setup of Fig. 1a. Interestingly, in the setup of Fig. 1b, the *total* cascaded contribution does not depend on the orientation of the sample. Note also that, in the setup of Fig. 1a, acoustic phonons contribute about 50% to $\chi^{(3),\mathrm{EFF}}_{3333}(c \parallel y)$ of $KNbO_3$ (which corresponds to more than a factor of 2 for the DFWM signal).

The total energy in the signal pulse in DFWM is $E_{\mathrm{sig}} = \zeta^2 \eta |\chi^{(3),\mathrm{EFF}}|^2$, where ζ is an unknown calibration factor that depends on difficult to control parameters such as beam profiles and overlap in the sample, η collects all known experimental quantities that affect the measurement, and $\chi^{(3),\mathrm{EFF}}$ is the active effective susceptibility coefficient.

For noncentrosymmetric materials the geometry dependencies showcased in Table I can be exploited, in place of a reference material with well known susceptibility, to determine the calibration factor ζ:

$$\zeta = \frac{(\sqrt{E_{\mathrm{sig}}/\eta})_z - (\sqrt{E_{\mathrm{sig}}/\eta})_y}{|\chi^{\mathrm{casc}}|_z - |\chi^{\mathrm{casc}}|_y}, \qquad (20)$$

where the subscripts z and y indicate two orientations of the sample with the same direct third-order contribution, and χ^{casc} is the sum of the two cascaded contributions in (9). This equation relates the variations in DFWM signal strength to the calculated cascaded contributions, and therefore the experimental values of the third-order susceptibilities to the linear electro-optic properties.

We applied this technique in the experimental geometry of Fig. 1a for $BaTiO_3$ and $KNbO_3$. The measurements were performed using $\chi^{(3)}_{2233}$ for the calibration and comparing the other coefficients to the $\chi^{(3)}_{2233}$ setup by taking into account the different light beam polarizations. $\chi^{(3)}_{2233}$ was chosen because of its large cascaded contributions and the absence of piezoelectric relaxation ($r_{ijk} = r^S_{ijk}$), which minimizes the influence of experimental errors and the number of material parameters that must be known.

The experimental susceptibility values we measured at 1.06 μm and for 100 ps pulses are, in units of $10^{-22}\ \mathrm{m^2/V^2}$, $\chi^{(3),\mathrm{EFF}}_{1133}(c \parallel y) = 560 \pm 80$, $\chi^{(3),\mathrm{EFF}}_{1133}(c \parallel z) = 340 \pm 80$ for $BaTiO_3$, and $\chi^{(3),\mathrm{EFF}}_{2233}(c \parallel y) = 330 \pm 70$, $\chi^{(3),\mathrm{EFF}}_{2233}(c \parallel z) = 190 \pm 50$ for $KNbO_3$. Note that the direct third-order contributions are only $\chi^{(3)}_{1133} \sim 110$ for $BaTiO_3$ and $\chi^{(3)}_{2233} \sim 60$ for $KNbO_3$. For the other coefficients, $\chi^{(3)}_{1111} \sim 160$, $\chi^{(3)}_{3333} \sim 100$ for $BaTiO_3$, and $\chi^{(3)}_{2222} \sim 180$, $\chi^{(3)}_{3333} \sim 60$ for $KNbO_3$. A more detailed discussion of these experimental results will be given elsewhere.

The results above were checked with a classical reference measurement. Comparing the experimental signal to the one observed with a 1 mm thick cell filled with CS_2, and using $\chi^{(3),\mathrm{CS_2}}_{1111} = 263 \pm 30$ [12], we got $\chi^{(3),\mathrm{EFF}}_{1133}(c \parallel y) = 550 \pm 100$ for $BaTiO_3$ and $\chi^{(3),\mathrm{EFF}}_{2233}(c \parallel y) = 290 \pm 60$ for $KNbO_3$.

This is in excellent agreement with the results obtained above using the cascading contributions in Table I as a reference, confirming the validity of the expressions and theoretical interpretations given in this paper.

In conclusion, we have demonstrated that DFWM in noncentrosymmetric materials requires special care in selecting experimental geometries in order to deliver reliable results, and we have shown how to calculate the geometry dependent second-order contributions for different pulse lengths. The second-order contributions can be exploited to calibrate a DFWM experiment and relate third-order susceptibilities to second-order dielectric and electro-optic properties experimentally.

[1] M. Zgonik and P. Günter, J. Opt. Soc. Am. B **13**, 570–576 (1996).
[2] P. D. Maker and R. W. Terhune, Phys. Rev. **137**, A801–A818 (1964).
[3] R. W. Hellwarth, Prog. Quantum Electron. **5**, 1–68 (1977).
[4] R. W. Hellwarth, J. Opt. Soc. Am **67**, 1 (1977).
[5] F. P. Strohkendl, L. R. Dalton, R. W. Hellwarth, H. W. Sarkas, and Z. H. Kafafi, J. Opt. Soc. Am. **14**, 92 (1997).
[6] P. N. Butcher and D. Cotter, *The Elements of Nonlinear Optics* (Cambridge University Press, Cambridge, 1991).
[7] Chr. Flytzanis and N. Bloembergen, Prog. Quantum Electron. **4**, 271–300 (1977).
[8] M. Zgonik, R. Schlesser, I. Biaggio, E. Voit, J. Tscherry, and P. Günter, J. Appl. Phys. **74**, 1287 (1993).
[9] F. I. Fedorov, *Theory of Elastic Waves in Crystals* (Plenum Press, New York, 1968).
[10] P. Bernasconi, M. Zgonik, and P. Günter, J. Appl. Phys. **78**, 2651 (1995).
[11] M. Zgonik, P. Bernasconi, M. Duelli, R. Schlesser, P. Günter, M. H. Garrett, D. Rytz, Y. Zhu, and X. Wu, Phys. Rev. B **50**, 5941–5949 (1994).
[12] N. Tang, J. P. Partanen, R. W. Hellwarth, and R. J. Knize, Phys. Rev. B **48**, 8404 (1993).